Effects of bacteria on CdS thin films used in technological devices

2017 Mater. Res. Express 4 046402

(http://iopscience.iop.org/2053-1591/4/4/046402)

Materials Research Express

PAPER

Effects of bacteria on CdS thin films used in technological devices

RECEIVED
23 January 2017

REVISED
21 March 2017

ACCEPTED FOR PUBLICATION
24 March 2017

PUBLISHED
12 April 2017

S Alpdoğan[1], A O Adıgüzel[2], B Sahan[3], M Tunçer[2] and H Metin Gubur[1,3]

[1] Department of Physics, Mersin University, 33343 Mersin, Turkey
[2] Department of Biology, Mersin University, 33343 Mersin, Turkey
[3] Advanced Technology Education, Research and Application Center, Mersin University, 3343 Mersin, Turkey

E-mail: soneralpdogan@gmail.com

Keywords: CdS, chemical bath deposition, bacteria effects

Abstract

Cadmium sulfide (CdS) thin films were fabricated on glass substrates by the chemical bath deposition method at 70 °C considering deposition times ranging from 2 h to 5 h. The optical band gaps of CdS thin films were found to be in the 2.42–2.37 eV range. CdS thin films had uniform spherical nano-size grains which had polycrystalline, hexagonal and cubic phases. The films had a characteristic electrical resistivity of the order of $10^5\Omega$ cm and n-type conductivity at room condition.

CdS thin films were incubated in cultures of *B.domonas aeruginosa* and *Staphylococcus aureus*, which exist abundantly in the environment, and form biofilms. SEM images showed that *S. aureus* and *K. pneumonia* were detected significantly on the film surfaces with a few of *P. aeruginosa* and *B. subtilis* cells attached. CdS thin film surface exhibits relatively good resistance to the colonization of *P. aeruginosa* and *B. subtilis*. Optical results showed that the band gap of CdS thin films which interacted with the bacteria is 2.42 eV. The crystal structure and electrical properties of CdS thin films were not affected by bacterial adhesion. The antimicrobial effect of CdS nanoparticles was different for different bacterial strains.

1. Introduction

Cadmium sulfide semiconductor thin films, which have a direct and wide band gap (2.42 eV at room condition) of the group of II–VI compounds, are being used as window materials for solar energy conversion, for fluorescence imaging and as biosensors for biological devices [1–11]. Due to the important applications, many researchers have fabricated CdS thin films by using different physical and chemical methods such as chemical bath deposition (CBD) [12–14], successive ionic layer adsorption and reaction method (SILAR) [15], spray pyrolysis [16], electrodeposition [17], thermal evaporation [18], sputtering [14] and molecular beam epitaxy [19]. Additionally, several researchers have prepared various morphologies of CdS semiconductors, for instance, nanowires, nanorods, nanorings, flakes, flowers, conifer-like and cauliflower-like microspheres [20–24] for improving the efficiency of the technological materials.

Microorganisms are widespread in different environments such as air, soil, river, sea and ocean and interact with biotic or abiotic surfaces. Microorganisms are present especially in the aqueous media attach to surfaces and colonize. Condensation of the atmospheric water on the dry surfaces create wet environment upon surfaces. This phenomenon leads to adhesion forces based on surface tension pressure differences [25]. Therefore, many microorganisms, especially those having the biofilm forming ability, can adhere, colonize and form biofilms on dry surfaces such as metals and thin films [26]. In this situation, important changes in pH values, ion types and concentration, dissolved oxygen concentration occur at metal surface/biofilm interfaces and cause damage on the surface of materials known as biocorrosion. Initial attachment of microorganisms is believed to be important for the colonization on the surface of materials [27]. However, many inorganic compounds can strongly resist microorganisms, for instance, Thomas *et al* [28] studied the antibacterial activity of pure and cadmium doped zinc oxide thin films. Jeon *et al* [29] reported the antibacterial activity of highly silver-doped silica thin films and they demonstrated excellent antibacterial performances of silver-doped silica thin films against *Escherichia coli* and *Staphylococcus aureus*. Also, antibacterial capabilities of CdS thin films against Gram-positive and Gram-negative bacteria were studied [30].

In this paper, CdS thin films with roughly between 80 − 195 nm thicknesses were fabricated on glass substrates using CBD at 70 °C. A set of the fabricated films were incubated with bacteria including *Bacillus subtilis*, *Klebsiella pneumonia*, *Pseudomonas aeruginosa* and *S. aureus*. Subsequently, adhesion and colonization of bacteria on film surfaces was evaluated. Additionally, the optical, morphological, electrical properties and the crystal structure of these CdS thin films which interacted and non-interacted with bacteria, were compared. Antimicrobial effect of the CdS nanoparticles used for producing CdS thin films was also determined.

2. Experimental processes

2.1. CdS thin films fabrication

The semiconductor CdS thin films were deposited on glass substrates by using CBD. The glass substrates were kept at an approximately 45 ° angle to the horizontal line in the beaker having a mixed deposition solution (0.015 M cadmium sulphate, 0.5 M hydrazine, 1 M thiourea and 25% NH_3 and double-distilled water) without stirring at 70 ± 2 °C for an hour. These processes were repeated for 2, 3, 4 and 5 h to get smooth, uniform and thicker CdS thin films. Subsequently, CdS thin films were cleaned in distilled water and propanol to clear away the feebly attached CdS particles on the surface and dried in air [12].

2.2. Storage of bacterial strains

B. subtilis, *K. pneumonia*, *P. aeruginosa* and *S. aureus* were stored at −80 °C in 20% glycerol and maintained on nutrient agar medium containing 5 g l^{-1} pepton, 3 g l^{-1} meat extract and 12 g l^{-1} agar at + 4 °C until being used.

2.3. Adhesion study and disk diffusion test

Bacterial strains were precultivated in nutrient broth (5 g l^{-1} pepton, 3 g l^{-1} meat extract) at pH 7.0, 30 °C and 150 rpm shaking condition overnight. Approximately 1×10^6 bacterial cells were inoculated to fresh 50 ml nutrient broth and then thin films which were sterilized by 70% ethanol were placed in the liquid medium. After cultures were incubated at 30 °C, 150 rpm for 10 d, CdS thin films were washed slightly with distilled water and displayed with electron microscopy for detection of the adherent bacterial cells on CdS thin film surfaces.

Antimicrobial activity of CdS nanoparticles used for coating the film against *P. aeruginosa*, *S. aureus*, *K. pneumonia* and *B. subtilis* was performed by disk diffusion method. Bacterial strains were transferred into the nutrient broth medium and incubated at optimum growth temperature of the bacterial strain (30 °C for *B. subtilis* and 37 °C for others) overnight. The culture suspension (100 μl) containing 1×10^7 cells ml^{-1} was inoculated on Mueller–Hinton agar (2 g l^{-1} meat infusion, 17.5 g l^{-1} casein hydrolysate, 1.5 g l^{-1} starch) and spread. Filter paper was placed on the solid medium surface and then CdS nanoparticles were dropped on the filter. After incubation of the culture for 2 d, inhibition zone was determined and measured.

2.4. The characterization of CdS thin films

The structural studies of the CdS thin films which interacted and non-interacted with bacteria were completed using Bruker AXS Advance D8 diffractometer in the range of diffraction angle $10° \leqslant 2\theta \leqslant 60°$ in steps of 0.02 ° with 40 kV at 30 mA, $CuK_{\alpha 1}$ radiation ($\lambda = 1.5406$ Å). The surface morphologies of CdS thin films which interacted and non-interacted with bacteria were investigated utilizing a Zeiss-Supra 55 SEM equipped with an energy dispersive x-ray (EDX) spectrometer at various magnifications. The optical transmittance of the films were carried out using UV–visible spectrophotometer (Shimadzu UV − 1700) in the wavelength range of 400 − 700 nm at room conditions. Additionally, the resistivity, mobility and carrier concentration of the films were found using a Van der Pauw four-point probe configuration with a magnetic induction of 0.54 T in hall effect measurements system (HMS − 3000) at room conditions.

3. Results and discussion

3.1. The Properties of the CdS thin films

UV–visible spectrophotometer was used to obtain the optical properties (figure 1) such as transmission and band gap of the CdS thin films at room conditions. Figure 1(a) shows the transmission spectra recorded for wavelengths from 400 to 700 nm. Figure 1(a) displays the transmission spectra for different deposition hours and as seen from this figure, the films demonstrated highest transmittance in the visible wave lengths.

The optical band gap energy (E_g) was calculated from the equation of absorption coefficient, α:

$$\alpha = \frac{A(h\nu - E_g)^{1/2}}{h\nu}$$

where A is a constant, $h\nu$ is the photon energy. The optical band gap of CdS thin films were estimated by plotting $(\alpha h\nu)^2$ versus photon energy in figure 1(b). The optical band gap changed with deposition time of CdS thin films,

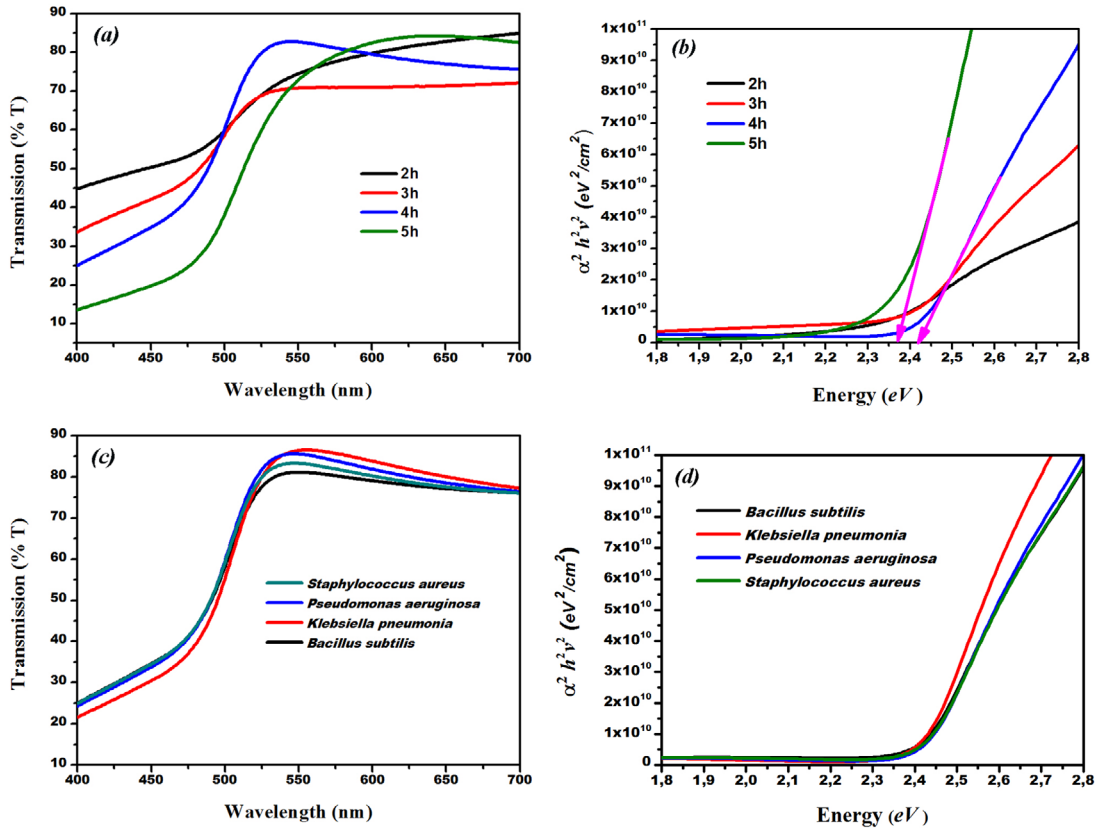

Figure 1. The transmittance versus wavelength of CdS thin films for (a) deposition time (c) the CdS thin films affected by bacteria and the $(\alpha hv)^2$ versus photon energy of CdS thin films for (b) deposition time (d) the CdS thin films affected by bacteria.

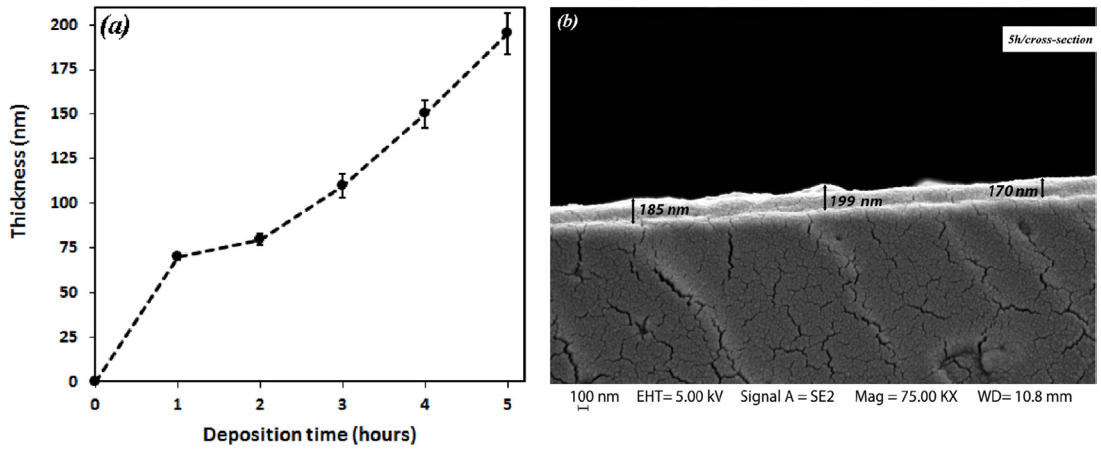

Figure 2. (a) The thickness versus deposition time for CdS thin films and (b) the cross-section SEM image for 5 h deposited CdS thin film.

from 2.42 ± 1 eV to 2.37 ± 1 eV, and the 4 h deposited CdS thin film had 2.42 ± 1 eV band gap which is the characteristic band gap of CdS thin films for bulk at room condition.

The optical thicknesses of the CdS thin films shown in figure 2(a) were determined from transmission interference using the following relation [31]:

$$d = \frac{1}{2n_1\Delta(1/\lambda)}$$

where d is the optical film thickness, n_1 is the refractive index and $1/\lambda$ is the wavenumber interval between two maxima or minima. It is seen from figure 2(a) that the optical thickness of CdS thin films increased with the deposition time of the film; approximately 80 ± 5, 110 ± 11, 150 ± 13 and 195 ± 15 nm, respectively. Also, these results are compared with the physical thickness of the 5 h deposited CdS thin film in the SEM image of figure 2(b).

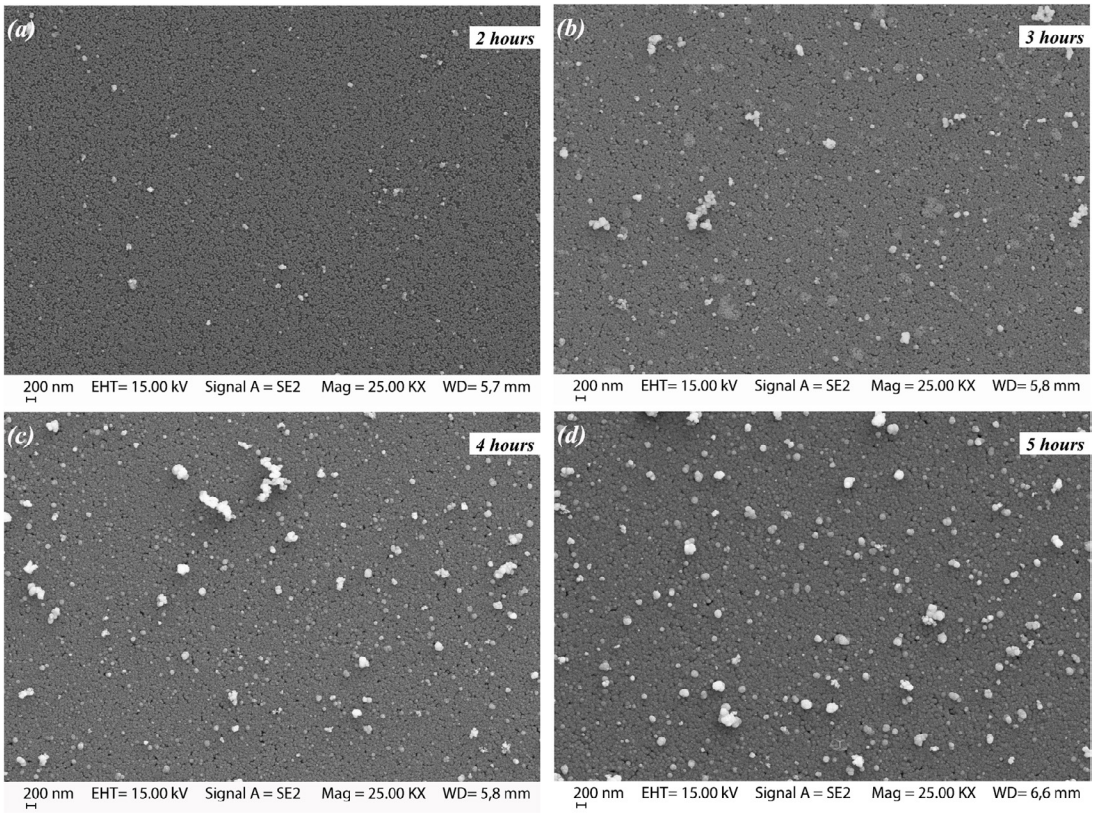

Figure 3. The SEM images of CdS thin films for deposition times of (a) 2 h (b) 3 h (c) 4 h (d) 5 h.

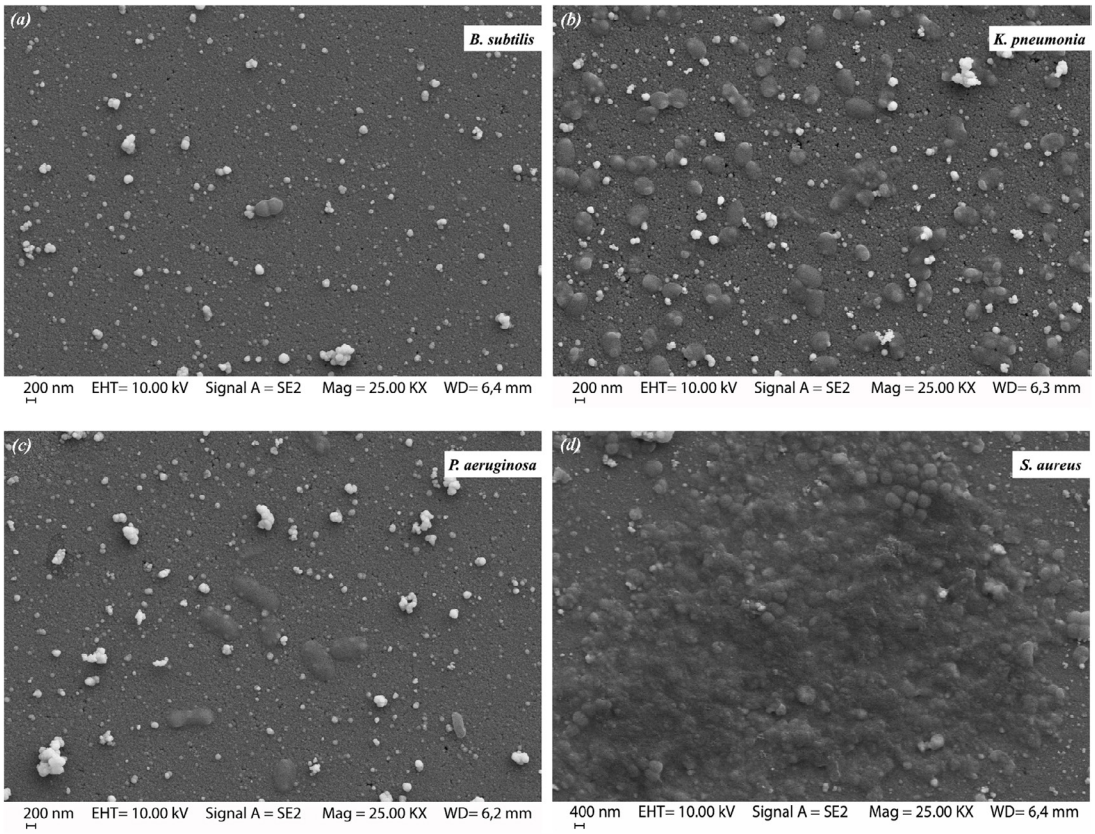

Figure 4. The SEM images of the CdS thin films affected by bacteria (a) *B. subtilis* (b) *K. pneumonia* (c) *P. aeruginosa* (d) *S. aureus*.

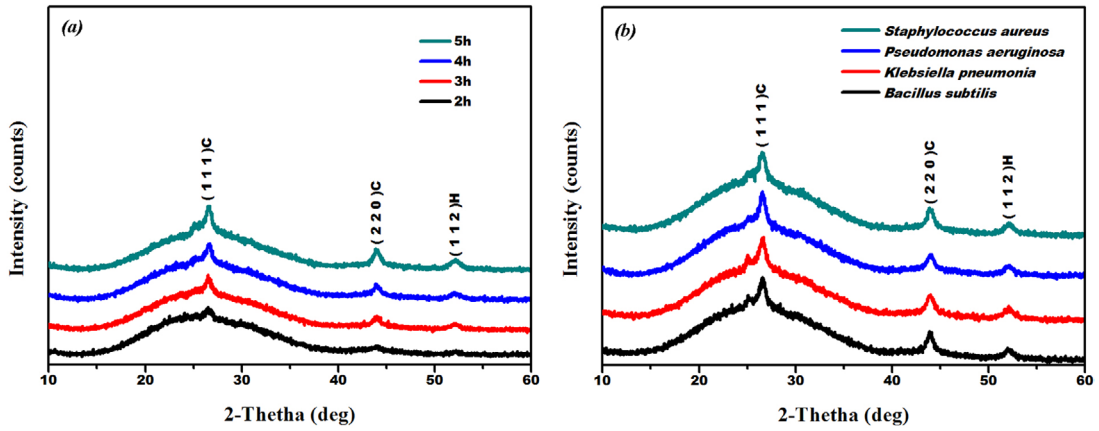

Figure 5. X-ray diffractograms of films of CdS thin films for (a) deposition time (b) affected by bacteria.

Table 1. The FWHM, crystallite size, dislocation density, number of the crystallites/unit area, and strain of CdS thin films.

CdS Samples (h)	FWHM β (rad) (10^{-2})	Crystallites size (nm)	Dislocation density (10^{15} lines m^{-2})	Number of crystallites/ unit area (10^{17} m^{-2})	Strain (10^{-4})
2	~8.4	~1.7	~345	~162	~200
3	~2.7	~5.3	~36	~7.5	~66
4	~1.1	~12.5	~5.9	~0.75	~28
5	~1.0	~13.9	~5.2	~0.73	~25

Table 2. The FWHM, crystallite size, dislocation density, number of the crystallites/unit area, and strain of the CdS thin films affected by bacteria.

Bacteria	FWHM β (rad) (10^{-2})	Crystallites size (nm)	Dislocation density (10^{15} lines m^{-2})	Number of crystallites/ unit area (10^{17} m^{-2})	Strain (10^{-4})
B. subtilis	~1.1	~12.5	~6.3	~0.75	~27.6
K. pneumonia	~1.1	~12.5	~6.3	~0.75	~27.6
P. aeruginosa	~1.1	~12.7	~6.1	~0.72	~26.1
S. aureus	~1.1	~12.7	~6.1	~0.72	26.1

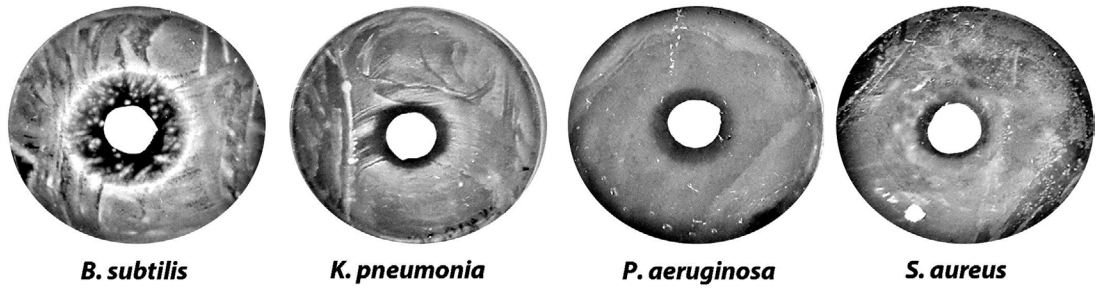

Figure 6. The antimicrobial effect of CdS nanoparticles against bacteria, *B. subtilis*, *K. pneumonia*, *P. aeruginosa* and *S. aureus*.

Figure 3 demonstrates the SEM images of the increasing deposition time for CdS thin films. The grain size of the uniform spherical nano-sized particles remarkably grew up with the increasing deposition time of the CdS thin films and consequently, the boundaries between the grains decreased as shown in the images of figure 3.

The XRD patterns of the CdS thin films are shown figure 5(a). As seen, XRD patterns of the CdS thin films had cubic (C) and hexagonal (H), (1 1 1)C, (2 2 0)C and (1 1 2)H, phases which were identified with reference patterns (JCPDS NO: 01-079-6256, 01-74-9664). The intensity of peaks increased with the deposition time of the film as shown in figure 5(a). The crystal planes of CdS thin films did not change with the increasing deposition time of CdS thin films. The crystallite size, the dislocation densities (crystallographic defect, or irregularity, within a crystal structure), the number of crystallites/unit area and the strains (surface deformation) of CdS thin films were calculated from the full width at half maximum (FWHM) of (1 1 1)C peak phase by considering the Debye–Scherrer formula [12] in table 1. It is clearly seen from table 1 that the crystallite size grew up with the increasing

deposition time of CdS thin films, while the FWHM, the surface deformation, the number of crystallites/unit area and crystallographic defect, or irregularities within a crystal structure decreased. The growth of grain size is also seen in the SEM images of figure 3.

The resistivity of CdS thin films was obtained by Hall effect measurements at room conditions. CdS thin films had $\sim 4 \times 10^5\,\Omega$ cm electrical resistivity which is the characteristic electrical resistivity of the semiconductor thin films (of the order of $10^{-2} - 10^9\,\Omega$ cm) at room conditions and the conductivity type of the CdS thin films is n-type.

3.2. The Properties of the CdS thin films affected by bacteria and antimicrobial properties of the CdS nanoparticles

Various bacterial strains were obtained from the repository at Medical Center and soil related to rhizosphere. Among these, four different biofilm forming isolates were selected according to Carlos *et al* [32] for further tests and identified as *P. aeruginosa*, *S. aureus*, *K. pneumonia* and *B. subtilis* according to the morphological and biochemical characteristics. *B. subtilis* cells which are known to form endospores for survival in extreme environmental conditions, had the lowest cells attached on CdS thin film surface among the four bacterial strains (figure 4). Although *P. aeruginosa* adhered more than *B. subtilis*, no colonization was observed. The number of viable cells of *K. pneumonia* on CdS film surface was higher. But, *S. aureus* cells were found to have a greater propensity for attachment to surfaces of CdS thin films. Also, *S. aureus* colonized and slightly formed biofilms on the film surface. Similarly, high adhesion propensity of *S. aureus* was reported previously [33]. Attachment propensity to the CdS thin film varied with the bacterial strain. Figures 1(c) and (d) show the transmittance and optical band gaps of the CdS thin films affected by bacteria: optical results showed that the band gap of CdS thin films affected by bacteria is 2.42 ± 1 eV which means that the films band gap was not changed by the interaction with the bacterial cells. It is seen from figure 5(b) that neither the crystal planes of the CdS thin films nor the intensity of the peaks changed, even if the bacteria were attached on the film surface and also, the calculated results of XRD data approximately had the same results for the CdS thin film affected by the bacteria as seen in table 2. Consequently, the attachment and colonization of the bacteria on the film surface did not cause any defect or disruption in the crystal structure of the films. Also, the resistivity properties of CdS thin films ($\sim 4 \times 10^5\,\Omega$ cm) did not change with the interaction of the bacteria and growth of biofilms on the films.

Disk diffusion method showed that CdS nanoparticles exhibited higher antimicrobial effect against *B. subtilis* while minimum inhibition zone diameter was observed for *S. aureus*. Disk diffusion study also showed revealed that the attachment potential of the bacterial strains could alter depending on the antimicrobial effect of the CdS nanoparticles against bacteria (figure 6).

4. Conclusions

CdS thin films were fabricated on glass substrates by CBD using deposition times ranging from 2 h to 5 h at 70 ± 2 °C. The effects of the deposition time and annealing temperatures of the CdS thin films on the optical, morphological, quantitative elemental, crystallite and electrical properties of the films were discussed. The obtained results showed that the increasing deposition time led to the enhancement of the good CdS thin films having the proper energy band gap ($2.42 - 2.37$ eV), convenient crystal structure (less crystallographic defects or irregularities) and characteristic electrical resistivity ($\sim 4 \times 10^5\,\Omega$ cm at room conditions).

The effects of bacteria, namely *B. subtilis*, *K. pneumonia*, *P. aeruginosa* and *S. aureus*, which exist abundantly in different habitats such as aquatic and terrestrial environments were investigated on the fabricated 4 h deposited CdS thin films. *B. subtilis* did not attach to the film surfaces, whereas *K. pneumonia, P. aeruginosa* and *S. aureus* attached. The optical, morphological, electrical properties and the crystal structure of the CdS thin films affected by bacteria did not change, as the bacteria attached to surface. Therefore, we can say that the characteristic properties of the CdS thin films did not change as the bacteria formed biofilms on the surface.

Acknowledgments

We would like to thank to Mersin University, which granted this research through Mersin University Scientific Research Unit (contract no: 2015-TP3-1322).

References

[1] Wang D, Li D, Guo L, Fu F, Zhang Z and Wei Q 2009 Template-free hydrothermal synthesis of novel three-dimensional dendritic CdS nanoarchitectures *J. Phys. Chem.* C **113** 5984–90

[2] Deivanayaki S, Jayamurugan P, Mariappan R and Ponnuswamy V 2010 Optical and structural characterization of CdTe thin films by chemical bath deposition technique *Chalcogenide Lett.* **7** 159–63

[3] Song G, Zhang H, Li J, Peng Z, Li X and Chen L 2012 Poly (vinyl-pyrrolidone) assisted hydrothermal synthesis of flower-like CdS nanorings *Polym. Bull.* **68** 2061–9
[4] Kosyachenko L and Toyama T 2014 Current–voltage characteristics and quantum efficiency spectra of efficient thin-film CdS/CdTe solar cells *Sol. Energy Mater. Sol. Cells* **120** 512–20
[5] Echendu O K and Dharmadasa I M 2015 Graded-bandgap solar cells using all-electrodeposited ZnS, CdS and CdTe thin-films *Energies* **8** 4416–35
[6] Wondmagegn W, Mejia I, Salas-Villasenor A, Stiegler H J, Quevedo-Lopez M A, Pieper R J and Gnade B E 2016 CdS thin film transistor for inverter and operational amplifier circuit applications *Microelectron. Eng.* **157** 64–70
[7] Zhang H R, Xu J J and Chen H Y 2013 Electrochemiluminescence ratiometry: a new approach to DNA biosensing *Anal. Chem.* **85** 5321–5
[8] Bu Y, Chen Z, Li W and Yu J 2013 High-efficiency photoelectrochemical properties by a highly crystalline CdS-sensitized ZnO nanorod array *ACS Appl. Mater. Interfaces* **5** 5097–104
[9] Li H, Li M, Shih W Y, Lelkes P I and Shih W H 2011 Cytotoxicity tests of water soluble ZnS and CdS quantum dots *J. Nanosci. Nanotechnol.* **11** 3543–51
[10] Zhao W W, Yu P P, Shan Y, Wang J, Xu J J and Chen H Y 2012 Exciton-plasmon interactions between CdS quantum dots and Ag nanoparticles in photoelectrochemical system and its biosensing application *Anal. Chem.* **84** 5892–7
[11] Wang J, Zhao W W, Tian C Y, Xu J J and Chen H Y 2012 Highly efficient quenching of electrochemiluminescence from CdS nanocrystal film based on biocatalytic deposition *Talanta* **89** 422–6
[12] Ozcan G C, Gubur H M, Alpdogan S and Zeyrek B K 2016 The investigation of the annealing temperature for CdS cauliflower-like thin films grown by using CBD *J. Mater. Sci., Mater. Electron.* **27** 12148–54
[13] Thanihaichelvan M, Sockiah K, Balashangar K and Ravirajan P 2015 Cadmium sulfide interface layer for improving the performance of titanium dioxide/poly (3-hexylthiophene) solar cells by extending the spectral responsei *J. Mater. Sci., Mater. Electron.* **26** 3558–63
[14] Premarani R, Devadasan J J, Saravanakumar S, Chandramohan R and Mahalingam T 2015 Structural, optical and magnetic properties of Ni-doped CdS thin films prepared by CBD *J. Mater. Sci., Mater. Electron.* **26** 2059–65
[15] Sfaelou S, Sygellou L, Dracopoulos V, Travlos A and Lianos P 2014 Effect of the nature of cadmium salts on the effectiveness of CdS SILAR deposition and its consequences on the performance of sensitized solar cells *J. Phys. Chem.* C **118** 22873–80
[16] Yılmaz S, Töreli S B, Polat İ, Olgar M A, Tomakin M and Bacaksız E 2017 Enhancement in the optical and electrical properties of CdS thin films through Ga and K co-doping *Mater. Sci. Semicond. Process.* **60** 45–52
[17] Ojo A A, Salim H I, Olusola O I, Madugu M L and Dharmadasa I M 2017 Effect of thickness: a case study of electrodeposited CdS in CdS/CdTe based photovoltaic devices *J. Mater. Sci., Mater. Electron.* **28** 3254–63
[18] Jassim S A J, Zumaila A A R A and Al Waly G A A 2013 Influence of substrate temperature on the structural, optical and electrical properties of CdS thin films deposited by thermal evaporation *Results Phys.* **3** 173–8
[19] Okajima M and Tohda T 1992 Heteroepitaxial growth of MnS on GaAs substrates *J. Cryst. Growth* **117** 810–5
[20] Gao N and Guo F 2006 A hydrothermal approach to flake-shaped CdS single crystals *Mater. Lett.* **60** 3697–700
[21] Zhang H, Yang D and Ma X 2007 Synthesis of flower-like CdS nanostructures by organic-free hydrothermal process and their optical properties *Mater. Lett.* **61** 3507–10
[22] Zhu Z, Wu Y, Liu H, Chen G and Zhu C 2013 Synthesis of CdS cauliflower-like microspheres via a template-free hydrothermal method *Mater. Lett.* **107** 90–2
[23] Nan Y X, Chen F, Yang L G and Chen H Z 2010 Electrochemical synthesis and charge transport properties of CdS nanocrystalline thin films with a conifer-like structure *J. Phys. Chem.* C **114** 11911–7
[24] Kazeminezhad I, Hekmat N and Kiasat A 2014 Effect of growth parameters on structural and optical properties of CdS nanowires prepared by polymer controlled solvothermal route *Fibers Polym.* **15** 672–9
[25] Chung E, Kweon H, Yiacoumi S, Lee I, Joy D C, Palumbo A V and Tsouris C 2009 Adhesion of spores of Bacillus thuringiensis on a planar surface *Environ. Sci. Technol.* **44** 290–6
[26] Videla H A and Herrera L K 2005 Corrosión de origen microbiológico: mirando al future *Int. Microbiol.* **8** 169–80
[27] Yuan S J and Pehkonen S O 2007 Microbiologically influenced corrosion of 304 stainless steel by aerobic pseudomonas NCIMB 2021 bacteria: AFM and XPS study *Colloids Surf.* B **59** 87–99
[28] Thomas D, Abraham J, Sunil C V, Augustine S and Dennis Thomas T 2014 Antibacterial activity of pure and cadmium doped ZnO thin film *Am. J. Pharm. Res.* **4** 1612–6
[29] Jeon H J, Yi S C and Oh S G 2003 Preparation and antibacterial effects of Ag–SiO_2 thin films by sol–gel method *Biomaterials* **24** 4921–8
[30] Abd-Elkader O H and Shaltout A A 2015 Characterization and antibacterial capabilities of nanocrystalline CdS thin films prepared by chemical bath deposition *Mater. Sci. Semicond. Process.* **35** 132–8
[31] Schroder D K 2006 *Semiconductor Material and Device Characterization* (New York: Wiley) pp 611–2
[32] Sánchez C J, Mende K, Beckius M L, Akers K S, Romano D R, Wenke J C and Murray C K 2013 Biofilm formation by clinical isolates and the implications in chronic infections *BMC Infect. Dis.* **13** 1
[33] Truong V K, Lapovok R, Estrin Y S, Rundell S, Wang J Y, Fluke C J and Ivanova E P 2010 The influence of nano-scale surface roughness on bacterial adhesion to ultrafine-grained titanium *Biomaterials* **31** 3674–83